Journal of Statistical Mechanics: Theory and Experiment

PAPER: QUANTUM STATISTICAL PHYSICS, CONDENSED MATTER, INTEGRABLE SYSTEMS

Renormalization of discrete-time quantum walks with a non-Grover coin

To cite this article: Stefan Boettcher and Joshua L Pughe-Sanford *J. Stat. Mech.* (2018) 033103

View the article online for updates and enhancements.

You may also like

- Critical phases in the raise and peel model
D A C Jara and F C Alcaraz
- Large deviations of a long-time average in the Ehrenfest urn model
Baruch Meerson and Pini Zilber
- Generalized time evolution of the homogeneous cooling state of a granular gas with positive and negative coefficient of normal restitution
Nagi Khalil

This content was downloaded from IP address 72.18.99.31 on 16/03/2026 at 01:50

Journal of Statistical Mechanics: Theory and Experiment
An IOP and SISSA journal

PAPER: Quantum statistical physics, condensed matter, integrable systems

Renormalization of discrete-time quantum walks with a non-Grover coin

Stefan Boettcher and Joshua L Pughe-Sanford

Department of Physics, Emory University, Atlanta, GA 30322, United States of America
E-mail: sboettc@emory.edu

Received 17 December 2017
Accepted for publication 14 February 2018
Published 21 March 2018

Online at stacks.iop.org/JSTAT/2018/033103
https://doi.org/10.1088/1742-5468/aab050

Abstract. We present an in-depth analytic study of discrete-time quantum walks driven by a non-reflective coin. Specifically, we compare the properties of the widely-used Grover coin $\mathcal{C}_{\mathrm{G}}$ that is unitary and reflective ($\mathcal{C}_{\mathrm{G}}^2 = \mathbb{I}$) with those of a 3×3 'rotational' coin $\mathcal{C}_{60}$ that is unitary but non-reflective ($\mathcal{C}_{60}^2 \neq \mathbb{I}$) and satisfies instead $\mathcal{C}_{60}^6 = \mathbb{I}$, which corresponds to a rotation by $60°$. While such a modification apparently changes the real-space renormalization group (RG) treatment, we show that nonetheless this non-reflective quantum walk remains in the same universality class as the Grover walk. We first demonstrate the procedure with $\mathcal{C}_{60}$ for a three-state quantum walk on a one-dimensional (*1d*) line, where we can solve the RG-recursions in closed form in a process providing exact solutions for some difficult non-linear recursions. Then, we apply the procedure to a quantum walk on a dual Sierpinski gasket (DSG), for which we ultimately reproduce the same results found for $\mathcal{C}_{\mathrm{G}}$, further demonstrating the robustness of the universality class.

Keywords: quantum computation, renormalisation group

© 2018 IOP Publishing Ltd and SISSA Medialab srl

1742-5468/18/033103+19$33.00

J. Stat. Mech. (2018) 033103

Contents

1. Introduction **2**

2. Quantum walk on the line **3**
2.1. RG for the quantum walk on the line 5
2.2. RG-analysis for the Grover coin 6
2.3. RG-analysis for the non-reflective coin 11

3. Quantum walk on the DSG **13**
3.1. Renormalization group 13
3.2. RG-analysis for the quantum walk with a Grover coin 15
3.2.1. Fixed-point analysis. 16
3.3. RG-analysis for a quantum walk with a non-reflective coin 17
3.3.1. Fixed-point analysis. 18

4. Conclusion **18**

References **19**

1. Introduction

Recent studies of quantum walks [1–5] using the real-space renormalization group (RG) [6, 7] have revealed the rich analytic structure of this quantum extension of classical random walks [8–11], in which the stochastic operator in the master equation describing the dynamics is replaced with a unitary operator. Profound new insights can be obtained, for example, for the asymptotic behavior of quantum search algorithms [12]. For either type of walk, it is fundamental to determine the spreading behavior of the probability density function (PDF) $\rho(\vec{x}, t)$, which predicts the likelihood of detecting a walk at time t at the site of distance $x = |\vec{x}|$ after starting at the origin. Asymptotically, the PDF obeys the scaling collapse with the scaling variable $x/t^{1/d_{\mathrm{w}}}$,

$$\rho(\vec{x}, t) \sim t^{-\frac{\mathrm{d}_f}{\mathrm{d}_{\mathrm{w}}}} f\left(x/t^{\frac{1}{d_{\mathrm{w}}}}\right), \tag{1}$$

where d_{w} is the walk-dimension and d_f is the fractal dimension of the network [13]. This scaling impacts many important observables, such as the mean-square displacement, $\langle x^2 \rangle_t \sim t^{2/d_{\mathrm{w}}}$ [14].

One purpose of the RG is the exploration of universality classes in the dynamics of physical systems [15]. It reveals how internal symmetries—and their breaking—may affect the large-scale behavior of the system. These methods have been adapted to explore the asymptotic scaling of random walks [10, 13, 16] and quantum walks [17, 18]. We have derived exact RG-flow equations for discrete-time ('coined') quantum walks on a number of complex networks [18, 19], and argued that the walk dimension d_{w} in equation (1) for a quantum walk with a Grover coin $\mathcal{C}_{\mathrm{G}}$ is always *half* of that

J. Stat. Mech. (2018) 033103

for the corresponding random walk, $d_{\mathrm{w}}^{Q} = \frac{1}{2}\, d_{\mathrm{w}}^{R}$, first based on numerical evidence [19] and later substantiated by analytic results [6, 7]. Furthermore, this RG can be used to determine the fact that the computational complexity of a Grover search algorithm [20] merely depends on the spectral dimension d_s of the network that represents the database on which the quantum search is conducted [12]. It was not obvious, however, whether such a result would survive the breaking of certain symmetries, such as the reflectivity of the Grover coin, $\mathcal{C}_{\mathrm{G}}^2 = \mathbb{I}$, that is a remnant of Grover's original conception [20] of a quantum walk on a mean-field, all-to-all network. Here, we present an exploration of the extent of the universality class by using a non-reflective coin $\mathcal{C}_{60}$ that is equally unitary but non-reflective ($\mathcal{C}_{60}^2 \neq \mathbb{I}$) and instead satisfies $\mathcal{C}_{60}^6 = \mathbb{I}$, amounting to a 60°-degree rotation in the coin-space of the quantum walker. To the best of our knowledge, this is the first study of a coined quantum walk with a non-reflective coin. We discuss in detail the seemingly significant changes for the RG the new coin entails by studying the solvable case of a walk on the *1d*-line before we extend those insights to the nontrivial case of a quantum walker on a dual Sierpinski gasket (DSG). Our findings, however, suggest that the scaling behavior is ultimately unaffected by this change in coin. Thus, as far as breaking reflection symmetry with this coin is concerned, the universality class of the Grover walk appears to be robust. Of course, there is an infinite amount of such unitary, non-reflective coins. However, considering the algebraic challenges posed by the quantum walk for the RG, $\mathcal{C}_{60}$, which is a simple permutation of $\mathcal{C}_{\mathrm{G}}$, provides many new insights with manageable algebraic effort.

Along the way, we also address several technical issues that arise for the first time in the real-space RG for walks. The RG for classical random walks is straightforward [16]: The Laplace-poles for normalized hopping parameters, as well as observables alike, impinge on a fixed point at $z = 1$ along the real z-axis to connect asymptotic scaling in space and time, as expressed by the walk dimension d_{w} defined in equation (1). In the case of a quantum walk, poles accumulate in wedges, either along the unit-circle in the complex-z plane for hopping parameters, or constrained on the circle for the unitary observables, leading to a distinct interpretation [6, 7]. While for the reflective Grover coins $\mathcal{C}_{\mathrm{G}}$, these poles still impinge on either or both of $z = \pm 1$, the use of the non-reflective coin $\mathcal{C}_{60}$ affords us the opportunity to explore the interpretation of situations where such poles impinge on fixed points at non-trivial z_0 on the unit-circle in model problems that are exactly solvable, i.e. the *1d*-line. We then test those interpretations for the DSG, where no such solution exists. We find that precise knowledge of z_0 is not required for the RG analysis, although isolated exceptional points seem to exist that must be avoided.

This paper is organized as follows: in section 2, we discuss the basic features of the RG, and compare the exact results for the quantum walk on the *1d*-line for both coins. In section 3, we apply the same scheme to analyze the non-trivial case of quantum walks on DSG. In section 4, we conclude with a summary and discussion of our results.

2. Quantum walk on the line

The time evolution of a quantum walk is governed by the discrete-time master equation [5]

J. Stat. Mech. (2018) 033103

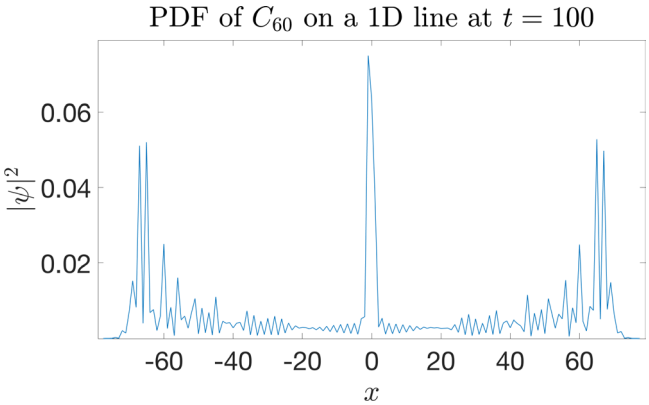

Figure 1. Snapshot of the probability density function $\rho(x,t) = \left|\psi^2_{x,t}\right|$ after $t = 100$ updates using $\mathcal{C}_{60}$ in equation (8) for a quantum walk starting from the origin. Quite similar to the equivalent walk with the Grover coin in equation (7) (see [21, 22]), this walk also exhibits a permanently localized component near its origin, while the remaining weight of the wave-function spreads ballistically in both directions along the lattice.

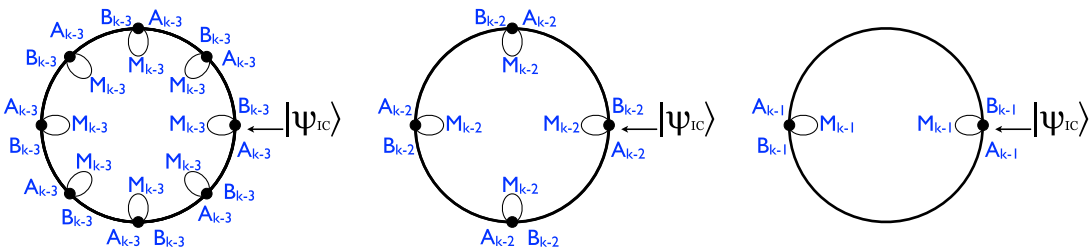

Figure 2. Depiction of the final three RG steps for a simple *1d*-line.

$$|\Psi_{t+1}\rangle = \mathcal{U}\,|\Psi_t\rangle \tag{2}$$

with unitary propagator $\mathcal{U}$. With $\psi_{x,t} = \langle x|\Psi_t\rangle$ in the discrete N-dimensional site-basis $|x\rangle$, the probability density function is given by $\rho(x,t) = \left|\psi^2_{x,t}\right|$. On this basis, the propagator can be represented as an $N \times N$ matrix $\mathcal{U}_{x,y} = \langle x\,|\mathcal{U}|\,y\rangle$ with operator-valued entries that describe the transitions between neighboring sites ('hopping matrices'). We can study the long-time asymptotics via a discrete Laplace transform,

$$\overline{\psi}_x(z) = \textstyle\sum_{t=0}^{\infty} \psi_{x,t} z^t, \tag{3}$$

as $|z| \to 1$ implies the limit $t \to \infty$ in a manner that we will have to specify. Then, equation (2) becomes

$$\overline{\psi}_x = z\mathcal{U}_{x,y}\overline{\psi}_y + \psi_{x,t=0}. \tag{4}$$

We review the time evolution of quantum walks on the *1d*-line for which the propagator in equation (2) is

$$\mathcal{U} = \textstyle\sum_x \{A\,|x+1\rangle\,\langle x| + B\,|x-1\rangle\,\langle x| + M\,|x\rangle\,\langle x|\} \tag{5}$$

for nearest-neighbor transitions. The norm of ρ for quantum walks demands unitary propagation, $\mathbb{I} = \mathcal{U}^\dagger\mathcal{U}$, which then imposes the conditions $\mathbb{I}_r = A^\dagger A + B^\dagger B + M^\dagger M$ and

J. Stat. Mech. (2018) 033103

$0 = A^\dagger M + M^\dagger B = A^\dagger B$, consistent with $A + B + M$ being unitary. As there are no non-trivial choices for scalar solutions of the unitarity constraints, one extends Hilbert space to include an internal degree of freedom for the wave-function, the so-called coin-space, similar to giving the walker a spin. Often, one defines the propagator then as $\mathcal{U} = \mathcal{S}\,(\mathbb{I}_N \otimes \mathcal{C})$, with 'coin' $\mathcal{C}$ and 'shift' $\mathcal{S}$. The quantum walk entangles spatial and coin-degrees of freedom. First, the coin mixes all components of $\psi_{x,t}$, then the shift-matrices $S^{\{A,B,M\}}$ facilitate the subsequent transition to neighboring sites or the same site, respectively. We thus obtain the hopping matrices $A = S^A\mathcal{C}$, $B = S^B\mathcal{C}$, and $M = S^M\mathcal{C}$ with $S^A + S^B + S^M = \mathbb{I}$. Because the most general 2D unitary coin is also always reflective (aside from a trivial rotation) [17], to allow for a non-reflective coin requires at least a 3D coin-space, for which it is convenient to choose

$$S^A = \begin{bmatrix} 1 & 0 & 0 \\ 0 & 0 & 0 \\ 0 & 0 & 0 \end{bmatrix}, \quad S^B = \begin{bmatrix} 0 & 0 & 0 \\ 0 & 1 & 0 \\ 0 & 0 & 0 \end{bmatrix}, \quad S^M = \begin{bmatrix} 0 & 0 & 0 \\ 0 & 0 & 0 \\ 0 & 0 & 1 \end{bmatrix}. \tag{6}$$

Such a three-state quantum walk on the 1d-line has been investigated previously for a 3×3 Grover coin [21, 22],

$$\mathcal{C}_{\mathrm{G}} = \frac{1}{3}\begin{bmatrix} -1 & 2 & 2 \\ 2 & -1 & 2 \\ 2 & 2 & -1 \end{bmatrix}. \tag{7}$$

While the 3D coin attains the same asymptotic scaling as the more widely studied 2D case, it adds the interesting new aspect of localization to the dynamics [21, 22], where the walker becomes eternally confined near its starting site with a finite probability. In the following, we will investigate the effects of a non-reflective coin,

$$\mathcal{C}_{60} = \frac{1}{3}\begin{bmatrix} 2 & 2 & -1 \\ -1 & 2 & 2 \\ 2 & -1 & 2 \end{bmatrix}. \tag{8}$$

As the geometry is simple, it is not too surprising that we find qualitatively the same phenomenology for both coins, as shown in figure 1. Thus, we will not bother with the canonical Fourier solution of the problem that has been discussed for the Grover coin elsewhere [21, 22]. Instead, we will immediately proceed in treating this problem as an exactly solvable example for the RG from which we can glean insights on how to treat more complicated non-Grover quantum walks with RG.

2.1. RG for the quantum walk on the line

Inserting $\mathcal{U}$ in equation (5) into the transformed master equation (4) readily obtains $\overline{\psi}_x = zM\overline{\psi}_x + zA\overline{\psi}_{x-1} + zB\overline{\psi}_{x+1}$, which is the starting point for the RG. For simplicity, we consider the walk problem here with initial conditions (IC) localized at the origin, $\psi_{x,t=0} = \delta_{x,0}\psi_{IC}$. As depicted in figure 2, we recursively eliminate $\overline{\psi}_x$ for all sites for which x is an odd number, then set $x \to x/2$ and repeat, step-by-step for $k = 0, 1, 2, \ldots$. Starting at $k = 0$ with the 'raw' hopping matrices $A_0 = zA$, $B_0 = zB$, and $M_0 = zM$, after each step, the master equation becomes *self-similar* in form when redefining the

J. Stat. Mech. (2018) 033103

renormalized hopping matrices A_k, B_k, M_k. For example, near any even site x at step k we have [17]:

$$\begin{aligned}\overline{\psi}_{x-1} &= M_k\overline{\psi}_{x-1} + A_k\overline{\psi}_{x-2} + B_k\overline{\psi}_x,\\ \overline{\psi}_x &= M_k\overline{\psi}_x + A_k\overline{\psi}_{x-1} + B_k\overline{\psi}_{x+1} + \delta_{x,0}\psi_{IC},\\ \overline{\psi}_{x+1} &= M_k\overline{\psi}_{x+1} + A_k\overline{\psi}_x + B_k\overline{\psi}_{x+2}.\end{aligned} \tag{9}$$

Solving this *linear* system for site x yields $\overline{\psi}_x = M_{k+1}\overline{\psi}_x + A_{k+1}\overline{\psi}_{x-2} + B_{k+1}\overline{\psi}_{x+2}$ with RG 'flow'

$$\begin{aligned}A_{k+1} &= A_k\left(\mathbb{I} - M_k\right)^{-1} A_k, \qquad B_{k+1} = B_k\left(\mathbb{I} - M_k\right)^{-1} B_k,\\ M_{k+1} &= M_k + A_k\left(\mathbb{I} - M_k\right)^{-1} B_k + B_k\left(\mathbb{I} - M_k\right)^{-1} A_k.\end{aligned} \tag{10}$$

The purpose of the real-space RG then is to relate the asymptotic scaling of these recursions with $k \to \infty$ to the corresponding scaling of $|z| \to 1$ such that the results become scale-invariant. Note that rescaling in k refers to the rescaling length, while rescaling the Laplace variable z refers to rescaling in time via equation (3). In a nutshell, the rescaling of hopping matrices in equation (10), which depends on z, answers the question: If we start a walk in the center of a table of size $L_k = 2^k$ and it takes a typical time T_k to fall off, how much do we need to rescale that time $T_{k+1} = \lambda T_k$ when we double the size of the table, $L_{k+1} = 2L_k$?

2.2. RG-analysis for the Grover coin

For a quantum walk with the Grover coin $\mathcal{C}_{\mathrm{G}}$ in equation (8), we evolve equation (10) for a few iterations from its unrenormalized values [17]. Already after the first iteration, a recurring pattern emerges that suggests the ansatz $A_k = a_k S^A \mathcal{C}_{\mathrm{G}}$, $B_k = a_k S^B \mathcal{C}_{\mathrm{G}}$, and

$$M_k = \begin{bmatrix} 0 & b_k & 0\\ b_k & 0 & 0\\ 0 & 0 & z\end{bmatrix}\mathcal{C}_{\mathrm{G}}, \tag{11}$$

where at $k = 1$ the RG-flow becomes initiated with

$$a_{k=1} = \frac{z^2\left(z-1\right)}{z+3}, \quad b_{k=1} = \frac{2z^2\left(z+1\right)}{z+3}. \tag{12}$$

For this scalar parametrization with a_k and b_k, the RG-flow (10) closes after each iteration for

$$\begin{aligned}a_{k+1} &= \frac{a_k^2\left(z-1\right)}{\left(b_k-1\right)\left[\left(3z+1\right)b_k - z - 3\right]},\\ b_{k+1} &= b_k + \frac{a_k^2\left[\left(3z+1\right)b_k - 2z - 2\right]}{\left(b_k-1\right)\left[\left(3z+1\right)b_k - z - 3\right]}.\end{aligned} \tag{13}$$

These recursions have a non-trivial fixed point at $(a_\infty, b_\infty) = \left(\frac{1-z}{1+3z}, \frac{2(1+z)}{1+3z}\right)$, yet its Jacobian $J_\infty = \left.\frac{\partial(a_{k+1},b_{k+1})}{\partial(a_k,b_k)}\right|_{k\to\infty}$ is, in fact, z-independent and has a degenerate eigenvalue $\lambda_{1,2} = 2$. Note that we never had to specify a choice for z as the location of a

J. Stat. Mech. (2018) 033103

fixed point to arrive at this result. However, numerical iteration of the RG-flow in equation (13) from the initial conditions in equation (12) clearly shows that fixed points are only attained for very specific choices of z. Those values of z can be obtained by equating $(a_\infty, b_\infty) = (a_k, b_k)$, which provides an over-constraint condition when solving z. For instance, the initial conditions in equation (12) merely yield $z = \pm 1$ as fixed points for $k = 1$, $k = 2$ adds $z = -\left(2 \pm \mathrm{i}\sqrt{5}\right)/3$, etc. We will return to this issue later.

We note that the coined quantum walk presents entirely new issues when compared with a classical random walk [16]. Previously [6], it was observed that is not sufficient to consider the hopping parameters (a_k, b_k) alone. To study the true scaling behavior, actual observables need to be examined; although observables are functionals of the hopping parameters, they are constrained to be unitary, unlike the hopping parameters. As in the classical analysis of a random walk [16], there is an intimate connection between fixed points and the poles in the complex-z plane. The evolution under rescaling size (k) of those poles nearest to the fixed point yields the rescaling in time. In the classical case, poles only move along the real-z axis, and there is no distinction necessary between the scaling of the hopping parameters or physical observables. In the quantum walk, while those poles move both radially as well as tangentially along the unit-circle for hopping parameters, they are constrained to moving only strictly tangentially on the circle for a unitary observable. Thus, the largest Jacobian eigenvalue λ_1, uniquely relevant for the random walk, must be paired with the 2nd eigenvalue λ_2 to obtain the walk dimension [6]

$$d_{\mathrm{w}}^{Q} = \log_2 \sqrt{\lambda_1 \lambda_2}. \tag{14}$$

Hence, with $\lambda_1 = \lambda_2 = 2$, we obtain $d_{\mathrm{w}}^{Q} = 1$, as expected for a quantum walk on the *1d*-line. We proceed to a closer investigation of such an observable.

As shown in figure 2, the 1d-loop of $N = 2^k$ sites after $k-1$ RG-steps reduces to merely two sites:

$$\begin{aligned} \overline{\psi}_0 &= M_{k-1}\overline{\psi}_0 + (A_{k-1} + B_{k-1})\,\overline{\psi}_{\frac{N}{2}} + \psi_{IC}, \\ \overline{\psi}_{\frac{N}{2}} &= M_{k-1}\overline{\psi}_{\frac{N}{2}} + (A_{k-1} + B_{k-1})\,\overline{\psi}_0. \end{aligned} \tag{15}$$

By also eliminating the site $\overline{\psi}_{\frac{N}{2}}$, and utilizing the RG-recursions in equation (10), we obtain the amplitude at the origin $x = 0$ of a quantum walk, $\overline{\psi}_0 = X_k \psi_{IC}$, for the *1d*-line:

$$X_k = \left[\mathbb{I} - (A_k + B_k + M_k)\right]^{-1}. \tag{16}$$

It is now straightforward, from the expressions near equation (11), to express the observable X_k in terms of the hopping parameters (a_k, b_k):

$$X_k = \frac{\begin{bmatrix} \frac{-z-3+a_k(z-1)+2b_k(z+1)}{1+a_k-b_k} & \frac{-2a_k(z+1)-b_k(z-1)}{1+a_k-b_k} & -2a_k - 2b_k \\ \frac{-2a_k(z+1)-b_k(z-1)}{1+a_k-b_k} & \frac{-z-3+a_k(z-1)+2b_k(z+1)}{1+a_k-b_k} & -2a_k - 2b_k \\ -2z & -2z & a_k + b_k - 3 \end{bmatrix}}{(a_k + b_k)(3z+1) - (z+3)}. \tag{17}$$

It can prove additionally fruitful to first solve the RG-flow in equation (13) in closed form. A simple rational ansatz, amazingly, yields the *exact* solution to the non-linear, coupled system of equations in (13):

J. Stat. Mech. (2018) 033103

$$
\begin{aligned}
a_k &= \frac{(u-1)(z-1)(3uz+u-z-3)\,\xi^{2^{k-1}}}{(z-1)^2-(3uz+u-2z-2)^2\,\xi^{2^k}},\\
b_k &= \frac{u(z-1)^2-(3uz+u-2z-2)(2uz+2u-z-3)\,\xi^{2^k}}{(z-1)^2-(3uz+u-2z-2)^2\,\xi^{2^k}},
\end{aligned}
\tag{18}
$$

where the otherwise free constants u and ξ are fixed by the initial conditions at $k=1$ in equation (12):

$$
\begin{aligned}
\xi &= 16+9\cos(2\omega)+24\cos\omega-\cos\frac{\omega}{2}(6\cos\omega+4)\sqrt{18\cos\omega+6},\\
u &= \mathrm{e}^{\mathrm{i}\omega}\left[\frac{3}{2}\cos\omega-\frac{1}{2}+\frac{1}{2}\cos\frac{\omega}{2}\sqrt{18\cos\omega+6}\right],
\end{aligned}
\tag{19}
$$

using $z=\mathrm{e}^{\mathrm{i}\omega}$. Note that ξ is complex (with $|\xi|=1$) only for $\omega=\arg z\in I$ on the interval $I=\left(\pi-\arctan 2\sqrt{2},\pi+\arctan 2\sqrt{2}\right)$. An infinity of solutions for ω of $\xi^{2^j}=1$ for any integer $j\geqslant 0$ form a (likely dense) set of fixed points of the RG-flow on I, because they leave equation (18) invariant for all $j\leqslant k\leqslant\infty$.

It is instructive to define $\xi=\mathrm{e}^{\mathrm{i}\nu}$ and $u=\left[2(z+1)+\mathrm{i}\mathrm{e}^{\mathrm{i}\sigma}(z-1)\right]/(3z+1)$ to get

$$
\begin{aligned}
\cos\nu &= 9\cos(2\omega)+24\cos(\omega)+16,\\
\sin\sigma &= -\frac{9}{4}z^2-\frac{3}{2}z-\frac{5}{4}.
\end{aligned}
\tag{20}
$$

Then, the solution of the RG-flow given in equation (18) simplifies to

$$
\begin{aligned}
a_k &= \frac{(1-z)\cos\sigma}{(3z+1)\cos(2^k\nu+\sigma)},\\
b_k &= \frac{2(z+1)}{3z+1}+\frac{(z-1)\sin\left(2^k\nu\right)}{(3z+1)\cos(2^k\nu+\sigma)}.
\end{aligned}
\tag{21}
$$

From equation (17), we thus find

$$
X_k=\frac{\chi}{(z-1)\sin\left(2^{k-1}\nu\right)},
\tag{22}
$$

with a regular numerator matrix χ that does not have any k-dependent poles.

Note that the observable X_k in equation (22) has poles for $z=1$ and for real $\nu_n^{(k)}=n\pi/2^{k-1}$, $0\leqslant n<2^k$. By equation (20), however, ν can be real only for real $\omega=\arg z\in I$, i.e. on the corresponding segment of the unit-circle in the complex-z plane (where we furthermore have a uni-modular $\xi=\mathrm{e}^{\mathrm{i}\nu}$, $|\xi|=1$). The corresponding values for $\omega_n^{(k)}$ can be obtained from equation (20). Those Laplace-poles $\omega_n^{(k)}$ are shown in figure 3, obtained directly by iteration of the RG-flow for $k=1,\ldots,6$. The corresponding poles for the hopping parameters in equation (21) are at $\nu_m^{(k)}=(m\pi+1/2-\sigma)/2^{k-1}$, $0\leqslant m<2^k$, pushed slightly off the unit-circle by σ, as is generally the case [6]. There is clearly a connection between those poles and the aforementioned fixed points, as $2^k\nu_n^{(j)}$ for $k\geqslant j$ is always an integer multiple of 2π, such that the corresponding $\omega_n^{(j)}$ is also always a fixed point in equation (21). Thus, expanding an observable like X_k for large k (i.e. for any fixed point $\omega_n^{(j)}$ it is assumed that $k\gg j$) implies an expansion around such a pole, and one *generically* finds

J. Stat. Mech. (2018) 033103

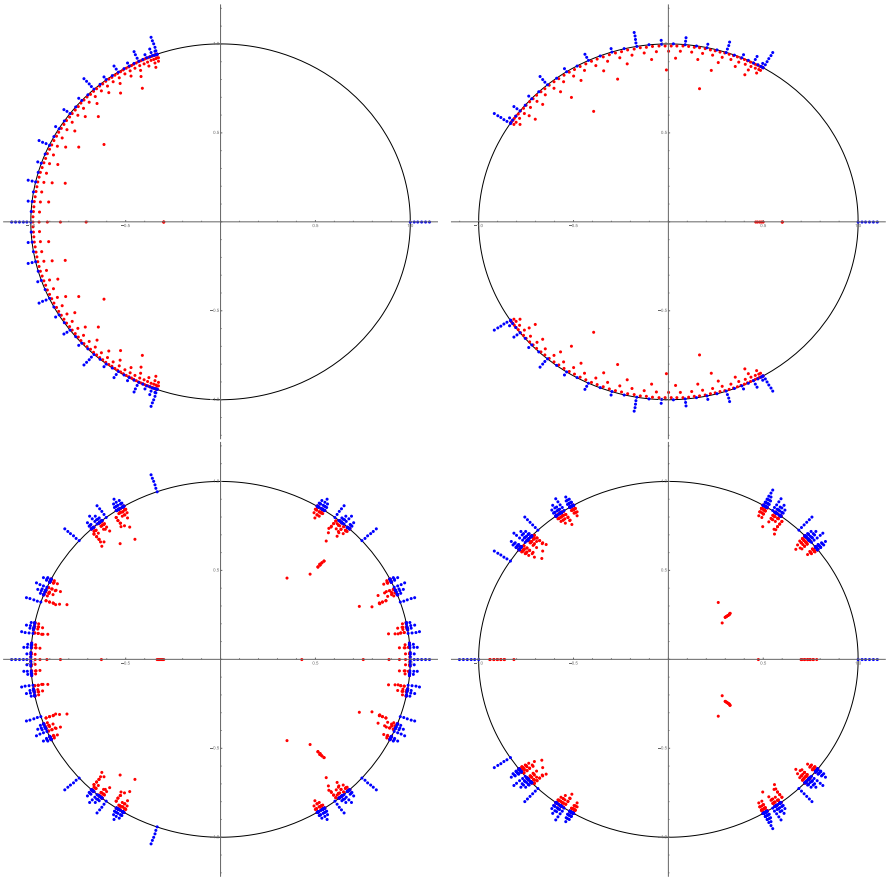

Figure 3. Plot of the poles of the Laplace transforms in the complex-z plane for the hopping parameters a_k and b_k (red points), and for the amplitude to remain at the origin, $\overline{\psi}_0^{(k)}(z) = X_k \psi_{IC}$ (blue points). The poles for the first few consecutive RG-steps are shown ($k = 1, \ldots, 6$) for a quantum walk on the $1d$-line (top) and DSG (bottom). On the left, the quantum walk is driven by the Grover coin in equation (7), and on the right, the rotational coin in equation (8) was applied. Since both coins are real, it is certain that poles will occur in complex-conjugate pairs. As X_k is unitary, all its poles are on the unit-circle (black line) in the complex-z plane; however, for better visibility, we have offset the poles increasingly outward for smaller k. Since the poles of the hopping parameters are all strictly outside (but converging onto) the unit-circle, we have applied the same offset but also mapped the poles (by $z \to 1/z$) to the inside. Note that if a pole for the observable arises at some k_0, it remains to be a pole for all $k \geqslant k_0$; this is not true for the hopping parameters. Generally, the pattern by which poles evolve appears more complicated for DSG. For walks with the Grover coin $\mathcal{C}_{\mathrm{G}}$, ever more poles progressively impinge on the real-z axis, at either of $z = \pm 1$, or both. For the non-reflective coin $\mathcal{C}_{60}$, the accumulation points for poles generally reside at non-trivial locations, for example at $\arg z = \pi \pm \arctan\sqrt{35}$ for the $1d$-line (top-right). Typically, the edges of the wedges within which poles accumulate represent fixed points that yield exponents for the classical random walk, such as at $\arg z = \pi \pm \arctan 2\sqrt{2}$ for the $1d$-line with a Grover coin (top-left), or at both, $\arg z = \pi \pm \arctan \frac{\sqrt{11}}{5}$ and $\arg z = \pm\frac{\pi}{3}$, for the $1d$-line with the non-reflective coin (top-right). The domains in which poles appear to become dense seem to break up like fractal Kantor-sets for the DSG.

J. Stat. Mech. (2018) 033103

$$X_k \sim \sum_{l=-1}^{\infty} \mathcal{M}_l \left(N\zeta\right)^l, \qquad \left(\zeta = z - z_{\mathrm{FP}} \to 0\right), \tag{23}$$

where we set $z_{\mathrm{FP}} = \mathrm{e}^{\mathrm{i}\omega_n^{(j)}}$, and all $\mathcal{M}_l\left(z_{\mathrm{FP}}\right)$ are matrices that become constant after neglecting higher-order corrections in inverse size $N = 2^k$ for each order in ζ. Although those constants vary with the choice of z_{FP}, they cannot affect the sought-after scaling behavior. Clearly, $z_{\mathrm{FP}} = -1$ is the most convenient (and symmetric—see figure 3) choice. The classical choice $z_{\mathrm{FP}} = 1$ would not work, even though $z = 1$ is a pole of X_k. However, that pole is isolated, as figure 3 shows, and we observe from equation (21) that $(a_k, b_k) = (0, 1)$ is trivial and without N-dependence in its expansion.

Finally, we study how these choices affect the asymptotic analysis of the RG-flow in equation (13). After all, and as we will see below, we are typically not in possession of the exact location of poles. In some elementary cases, such as the two-state quantum walk on a line [7], the RG-flow does not have an explicit z-dependence and the expansion around some z_{FP} remains purely formal, without any need for specificity. Even if z explicitly appears, such as in equation (13), we can replace $z = z_{\mathrm{FP}} + (z - z_{\mathrm{FP}}) \sim z_{\mathrm{FP}}$, since we are aiming to analyze an *unstable* fixed point with diverging corrections, which corrections in small $(z - z_{\mathrm{FP}})$ cannot provide. To wit, for a generic RG-flow $\vec{a}_{k+1}(z) = \mathcal{RG}\left(\vec{a}_k(z); z\right)$, expanded around the fixed point z_{FP} in the limit of large system sizes, $k \to \infty$, we have to linear order:

$$\vec{\alpha}_{k+1}(z) \sim \left[\vec{\alpha}_k \circ \vec{\nabla}_{\vec{a}} + (z - z_{\mathrm{FP}})\,\partial_z\right] \mathcal{RG}\left(\vec{a}_\infty(z_{\mathrm{FP}}); z_{\mathrm{FP}}\right) + \ldots, \tag{24}$$

with $\vec{\alpha}_k(z) = \vec{a}_k(z) - \vec{a}_\infty(z_{\mathrm{FP}})$ with $\vec{a}_\infty(z_{\mathrm{FP}}) = \mathcal{RG}\left(\vec{a}_\infty(z_{\mathrm{FP}}); z_{\mathrm{FP}}\right)$ defining the fixed point. It is then the divergent eigen-solutions $\{\lambda_i, \vec{v}_i\}$ of the Jacobian $J_\infty = \vec{\nabla}_{\vec{a}} \mathcal{RG}\left(\vec{a}_\infty(z_{\mathrm{FP}}); z_{\mathrm{FP}}\right)$, i.e. those with eigenvalues $\lambda_i > 1$, that dominate the solution for $k \to \infty$, while the k-independent inhomogeneity $(z - z_{\mathrm{FP}})\,\partial_z \mathcal{RG}\left(\vec{a}_\infty(z_{\mathrm{FP}}); z_{\mathrm{FP}}\right)$ remains irrelevant, to this and also in higher orders:

$$\vec{\alpha}_k(z) \sim \mathcal{A}\lambda_1^k \vec{v}_1 + \mathcal{B}\lambda_2^k \vec{v}_2 + \ldots. \tag{25}$$

In the case at hand in equation (13), we find that the Jacobian is already diagonal such that the eigenvectors are elementary, $\vec{v}_i = \widehat{e}_i$, with divergent eigenvectors $\lambda_1^k = \lambda_2^k = 2^k = N$, and we can insert:

$$\begin{aligned} a_k\left(z\right) &\sim a_\infty + \zeta\mathcal{A}\lambda_1^k + \zeta^2\alpha_k^{(2)} + \zeta^3\alpha_k^{(3)} + \ldots, \\ b_k\left(z\right) &\sim b_\infty + \zeta\mathcal{B}\lambda_2^k + \zeta^2\beta_k^{(2)} + \zeta^3\beta_k^{(3)} + \ldots, \end{aligned} \tag{26}$$

while simply setting $z = z_{\mathrm{FP}}$. We then find the most divergent terms in each order as:

$$\begin{aligned} \alpha_k^{(2)} &\sim \frac{1 + 3z_{\mathrm{FP}}}{2\left(1 - z_{\mathrm{FP}}\right)} \left[\left(\mathcal{A}\lambda_1^k\right)^2 + \left(\mathcal{B}\lambda_2^k\right)^2\right] + \ldots, \\ \alpha_k^{(3)} &\sim \frac{\left(1 + 3z_{\mathrm{FP}}\right)^2}{6\left(1 - z_{\mathrm{FP}}\right)^2} \left[\left(\mathcal{A}\lambda_1^k\right)^3 + 5\left(\mathcal{A}\lambda_1^k\right)\left(\mathcal{B}\lambda_2^k\right)^2\right] + \ldots, \\ \beta_k^{(2)} &\sim \frac{1 + 3z_{\mathrm{FP}}}{2\left(1 - z_{\mathrm{FP}}\right)} \left(\mathcal{A}\lambda_1^k\right)\left(\mathcal{B}\lambda_2^k\right) + \ldots, \\ \beta_k^{(3)} &\sim \frac{\left(1 + 3z_{\mathrm{FP}}\right)^2}{3\left(1 - z_{\mathrm{FP}}\right)^2} \left[2\left(\mathcal{A}\lambda_1^k\right)^2\left(\mathcal{B}\lambda_2^k\right) + \left(\mathcal{B}\lambda_2^k\right)^3\right] + \ldots. \end{aligned} \tag{27}$$

J. Stat. Mech. (2018) 033103

Inserted into X_k in equation (17), we indeed faithfully reproduce the expansion in equation (23), up to unknown (and irrelevant) constants. Not surprisingly, we find that the choice of z_{FP} does not affect the scaling results, except that $z_{\mathrm{FP}} = 1$ is excluded, consistent with the direct expansion of the exact solution.

2.3. RG-analysis for the non-reflective coin

We apply the same strategy for the quantum walk with the non-reflective coin $\mathcal{C}_{60}$ in equation (7): evolving equation (10) for a few iterations from its unrenormalized values [17], a recurring pattern emerges that suggests again the ansatz $A_k = a_k S^A \mathcal{C}_{60}$, $B_k = a_k S^B \mathcal{C}_{60}$, and

$$M_k = m_k \begin{bmatrix} 0 & \left(\frac{2-z}{2z-1}\right) b_k & 0 \\ b_k & 0 & 0 \\ 0 & 0 & z \end{bmatrix} \mathcal{C}_{60}. \tag{28}$$

Starting from

$$a_{k=1} = \frac{2z^2\,(z-1)}{2z-3}, \qquad b_{k=1} = \frac{z^2\,(1-2z)}{2z-3}, \tag{29}$$

the RG-flow now closes after each iteration for

$$\begin{aligned} a_{k+1} &= \frac{2\,(z-1)\,(2z-1)\,a_k^2}{(2z-3)(2z-1) - 2(z-2)(2z-1)b_k + (z-2)(3z-2)b_k^2}, \\ b_{k+1} &= b_k + \frac{2\,(2z-1)\,a_k^2\,[(3z-2)\,b_k - 2z + 1]}{(2z-3)(2z-1) - 2(z-2)(2z-1)b_k + (z-2)(3z-2)b_k^2}. \end{aligned} \tag{30}$$

Again, there is a close-form solution for the RG-flow:

$$\begin{aligned} a_k &= \frac{2\,(z-1)\,[(z-2)\,(3z-2)\,u^2 - 2\,(z-2)\,(2z-1)\,u + 4z^2 - 8z + 3]\,\xi^{2^{k-1}}}{4\,(2z-1)\,(z-1)^2 + (z-2)\,[(3z-2)\,u - 2z + 1]^2\,\xi^{2^k}}, \\ b_k &= \frac{2\,(z-1)\left\{4\,(z-1)^2\,u + [(z-2)\,u - 2z + 3]\,[(3z-2)\,u - 2z + 1]\,\xi^{2^k}\right\}}{4\,(2z-1)\,(z-1)^2 + (z-2)\,[(3z-2)\,u - 2z + 1]^2\,\xi^{2^k}}, \end{aligned} \tag{31}$$

where from equation (29) at $k = 1$ we obtain with $z = \mathrm{e}^{\mathrm{i}\omega}$:

$$\begin{aligned} \xi &= \frac{11}{8} + \frac{3}{2}\cos\omega + \frac{9}{4}\cos 2\omega - \frac{\sqrt{3}}{8}\,(1 + 6\cos\omega)\,\sqrt{1 + 4\cos\omega + 6\cos 2\omega}, \\ u &= \mathrm{e}^{\mathrm{i}\omega}\,\frac{2\cos\frac{\omega}{2} - 3\cos\frac{3\omega}{2} - \mathrm{i}\sqrt{3}\sin\frac{\omega}{2}\sqrt{1 + 4\cos\omega + 6\cos 2\omega}}{4\cos\omega - 5}. \end{aligned} \tag{32}$$

In agreement with equation (19), we note that ξ here is complex (with $|\xi| = 1$) for $\omega = \arg z \in I_\pm$ on the conjugate intervals $I_\pm = \left(\pm\frac{\pi}{3}, \pi \mp \arctan\frac{\sqrt{11}}{5}\right)$, leading to an infinity of solutions for ω of $\xi^{2^j} = 1$ for any integer $j \geqslant 0$ forming a (likely dense) set of fixed points of the RG-flow on $I_\pm$, because they leave equation (31) invariant for all $j \leqslant k \leqslant \infty$. As in the previous case for a Grover coin, Laplace poles of observables will be found to cluster on these intervals of the unit-circle in the complex-z plane

J. Stat. Mech. (2018) 033103

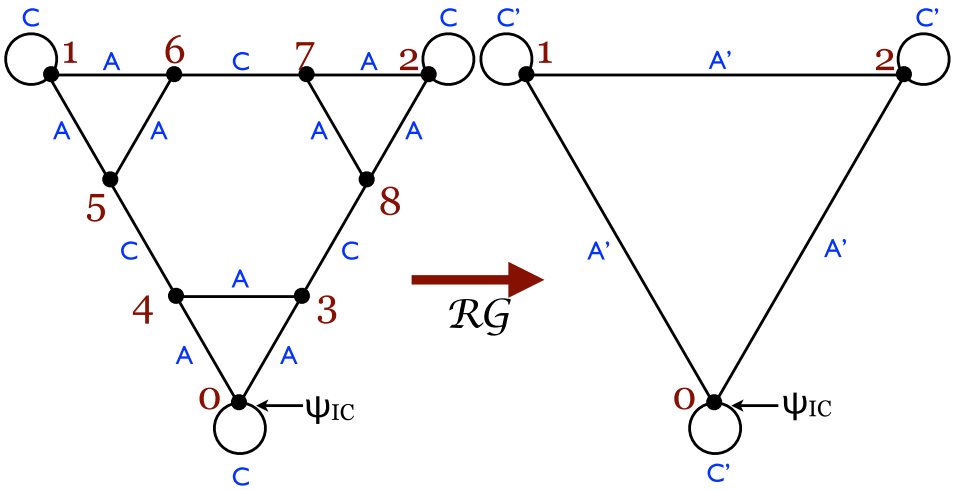

Figure 4. Depiction of the (final) RG-step in the analysis of DSG, as previously discussed in [7]. The letters $\{A, C\}$ label transitions between sites (black dots on the vertices) of the quantum walk in the form of hopping matrices. (Only on the three outermost sites does the matrix C refer back to the same site. For simplicity, we have omitted all such self-loops associated with hopping matrix M at each site.) Recursively, the inner-6 sites (labeled $3, \ldots, 8$) of each larger triangle (left) in DSG are decimated to obtain a reduced triangle (right) with renormalized hopping matrices (primed). To build a DSG of $N = 3^g$ sites, this procedure is applied (in reverse) g times to all triangles at each generation. Note that in each generation, the base-length L increases by a factor of $b = 2$, such that the fractal dimension is $d_\mathrm{f} = \log_{b=2} 3$.

(see figure 3). Most remarkable here is the fact that the real axes, i.e. $z = \pm 1$, are not inside those intervals. Extending this analysis to a new set of variables, $\xi = \mathrm{e}^{\mathrm{i}\nu}$ and $u = \frac{2(z-1)}{2-3z}\sqrt{\frac{2z-1}{z-2}}\mathrm{e}^{\mathrm{i}\sigma} + \frac{2z-1}{3z-2}$, we find, in agreement with equation (20):

$$\cos\nu = \frac{11}{8} + \frac{3}{2}\cos\omega + \frac{9}{4}\cos 2\omega, \qquad \sin\sigma = \frac{9z^3 - 3z^2 - z + 2}{4\sqrt{(2z-1)(2-z)}}. \tag{33}$$

In terms of these variables, we can conveniently express the solutions in equation (30) as

$$\begin{aligned} a_k &= \frac{2(z-1)\cos\sigma}{(3z-2)\cos(2^k\nu + \sigma)}, \\ b_k &= \frac{2z-1}{3z-2} + \frac{2(z-1)\sqrt{2z-1}\sin(2^k\nu)}{(3z-2)\sqrt{2-z}\cos(2^k\nu + \sigma)}. \end{aligned} \tag{34}$$

Using equation (16), we obtain the observable X_k, which in terms of equation (34), takes on the same form as in equation (22) (with an equivalent but numerically different matrix χ). All of a_k, b_k, and X_k appear very similar to their counterparts derived from the Grover coin in section 2.2, with poles of X_k for $z = 1$ and for real $\nu_n^{(k)} = n\pi/2^{k-1}$, $0 \leqslant n < 2^k$. In terms of the location of the poles in the complex-z plane, these values are attained via $\cos\nu$, as given in equations (20) and (33),

J. Stat. Mech. (2018) 033103

respectively. Accordingly, the $\nu_n^{(k)}$ are mapped onto the unit-circle with $\omega = \arg z$ in the intervals I and $I_\pm$, respectively, as shown in figure 3, knowledge of which would be essential to expand the exact X_k around some pole within the respective intervals. In contrast, the expansion of the RG-flow around some putative fixed point $z_{\rm FP}$, for either the non-reflective coin only or for the Grover coin in equation (26), is *oblivious* to the choice of $z_{\rm FP}$ in so far as the sought-after scaling behavior is concerned (i.e. aside from any numerical factors dependent on $z_{\rm FP}$, as in equation (27)). However, exceptional points may exist, such as the isolated pole at $z = 1$ in both examples, that should be avoided.

Despite the similarities in the analysis in both cases, the shift in poles away from the real-z axis could have signaled a change in universality classes for the quantum walk with these very distinct coins. Yet, in this simple example of a *1d*-walk, we find that both RG-flows provide identical eigenvalues for their Jacobians, leaving the walk dimension $d_{\rm w}^Q$ in equation (14) unchanged. In the following, we will apply these insights to the more involved (and not exactly solvable) RG-flow for a quantum walk on a DSG.

3. Quantum walk on the DSG

Basically, the same procedure as that in section 2.1—although algebraically more laborious—can be applied to obtain closed RG-recursions for a number of fractal networks [18, 19]. These have provided the first exact weak-limit results [22–24] for non-trivial networks beyond regular lattices. For completeness, we first briefly review the generic RG procedure for DSG here [7], before we address the specific physical situations posed by the reflective and non-reflective coins.

Due to the self-similarity of fractal networks, we can decompose $\mathcal{U}_{x,y}$ in equation (4) into its smallest sub-structure, exemplified by figure 4. It shows the elementary graphlet of nine sites that is used to recursively build the DSG of size $N = 3^g$ after g generations. The master equations pertaining to these sites are:

$$\begin{aligned}
\overline{\psi}_0 &= (M + C)\,\overline{\psi}_0 + A\left(\overline{\psi}_3 + \overline{\psi}_4\right) + \psi_{IC},\\
\overline{\psi}_{\{1,2\}} &= (M + C)\,\overline{\psi}_{\{1,2\}} + A\left(\overline{\psi}_{\{5,7\}} + \overline{\psi}_{\{6,8\}}\right),\\
\overline{\psi}_{\{3,4,5,6,7,8\}} &= M\overline{\psi}_{\{3,4,5,6,7,8\}} + C\overline{\psi}_{\{8,5,4,7,6,3\}} + A\left(\overline{\psi}_{\{0,3,1,5,2,7\}} + \overline{\psi}_{\{4,0,6,1,8,2\}}\right).
\end{aligned} \tag{35}$$

The hopping matrices A and C describe transitions between neighboring sites, while M permits the walker to remain on its site in a 'lazy' walk. The inhomogeneous ψ_{IC}-term allows for an initial condition $\psi_{x,t=0} = \delta_{x,0}\psi_{IC}$ for a quantum walker to start at site $x = 0$ in state ψ_{IC}.

3.1. Renormalization group

To accomplish the decimation of the sites $\overline{\psi}_{\{3,\ldots,8\}}$, as indicated in figure 4, we need to solve the linear system in equation (35) for $\overline{\psi}_{\{0,1,2\}}$. Thus, we expect that $\overline{\psi}_{\{3,\ldots,8\}}$ can be expressed as (symmetrized) linear combinations

J. Stat. Mech. (2018) 033103

$$\begin{aligned}\overline{\psi}_{\{3,4\}} &= P\overline{\psi}_0 + Q\overline{\psi}_{\{1,2\}} + R\overline{\psi}_{\{2,1\}},\\ \overline{\psi}_{\{5,8\}} &= R\overline{\psi}_0 + P\overline{\psi}_{\{1,2\}} + Q\overline{\psi}_{\{2,1\}},\\ \overline{\psi}_{\{6,7\}} &= Q\overline{\psi}_0 + P\overline{\psi}_{\{1,2\}} + R\overline{\psi}_{\{2,1\}}.\end{aligned} \tag{36}$$

Inserting this ansatz into equation (35) and comparing the coefficients consistently provides for the unknown matrices:

$$\begin{aligned}P &= (M+A)\,P + A + CR,\\ Q &= (M+C)\,Q + AR,\\ R &= MR + AQ + CP.\end{aligned} \tag{37}$$

Using the abbreviations $S = (\mathbb{I} - M - C)^{-1}A$ and $T = (\mathbb{I} - M - AS)^{-1}C$, equation (37) provides the solution:

$$P = (\mathbb{I} - M - A - CT)^{-1}\,A, \qquad R = TP, \qquad Q = SR. \tag{38}$$

Finally, after $\overline{\psi}_{\{3,\ldots,8\}}$ have been eliminated, we find

$$\begin{aligned}\overline{\psi}_0 &= ([M+2AP]+C)\,\overline{\psi}_0 + A\,(Q+R)\left(\overline{\psi}_1 + \overline{\psi}_2\right) + \psi_{IC},\\ \overline{\psi}_{\{1,2\}} &= ([M+2AP]+C)\,\overline{\psi}_{\{1,2\}} + A\,(Q+R)\left(\overline{\psi}_0 + \overline{\psi}_{\{2,1\}}\right).\end{aligned} \tag{39}$$

By comparing the coefficients between the renormalized expression in equation (39) and the corresponding *self-similar* expression in the first line of equation (35), we can identify the RG-recursions

$$\begin{aligned}M_{k+1} &= M_k + 2A_kP_k,\\ A_{k+1} &= A_k\,(Q_k + R_k)\,,\\ C_{k+1} &= C_k,\end{aligned} \tag{40}$$

where the subscripts refer to k- and $(k+1)$-renormalized forms of the hopping matrices. These recursions evolve from the un-renormalized ($k=0$) hopping matrices with $\{M, A, C\}_{k=0} = z\,\{M, A, C\}$. These RG-recursions are entirely generic and, in fact, would hold for any walk on DSG—classical or quantum. In the following, we now consider a specific form of a quantum walk with both the Grover coin in equation (7) as well as the non-reflective coin in equation (8).

As an observable, we focus again on $\overline{\psi}_0(z)$, the amplitude at the origin of the quantum walk on DSG, here chosen on one of the corner-sites. According to figure 4 and equation (39), we have

$$\begin{aligned}\overline{\psi}_0 &= (M_k + C_k)\,\overline{\psi}_0 + A_k\left(\overline{\psi}_1 + \overline{\psi}_2\right) + \psi_{IC},\\ \overline{\psi}_{\{1,2\}} &= (M_k + C_k)\,\overline{\psi}_{\{1,2\}} + A_k\left(\overline{\psi}_0 + \overline{\psi}_{\{2,1\}}\right),\end{aligned} \tag{41}$$

which has the solution $\overline{\psi}_0 = X_k\psi_{IC}$ with

$$X_k = \left[\mathbb{I} - M_k - C_k - 2A_k\,(\mathbb{I} - M_k - A_k - C_k)^{-1}\,A_k\right]^{-1}. \tag{42}$$

Preserving the norm of the quantum walk demands unitary propagation, i.e. $\mathbb{I} = \mathcal{U}^\dagger\mathcal{U}$. In [12], we have obtained generalized unitarity conditions for DSG as shown in figure 4:

J. Stat. Mech. (2018) 033103

$$\begin{aligned}\mathbb{I} &= 2A^\dagger A + C^\dagger C + M^\dagger M,\\ 0 &= A^\dagger A + A^\dagger M + M^\dagger A = C^\dagger M + M^\dagger C = A^\dagger C.\end{aligned} \tag{43}$$

3.2. RG-analysis for the quantum walk with a Grover coin

In this section, we review the behavior of a coined quantum walk on the DSG with the Grover-coin $\mathcal{C}_\mathrm{G}$ in equation (7), adapting the analysis from [7]. To study the scaling solution for the spreading quantum walk according to equation (1), as expressed by the walk dimension in equation (14), it is sufficient to investigate the properties of the RG-recursion in the previous section for $\{M, A, C\}$. In the unrenormalized ('raw') description of the walk, these hopping matrices are chosen as

$$M = \begin{bmatrix} -\frac{1}{3} & 0 & 0 \\ 0 & -\frac{1}{3} & 0 \\ 0 & 0 & 0 \end{bmatrix} \mathcal{C}_\mathrm{G}, \quad A = \begin{bmatrix} \frac{2}{3} & 0 & 0 \\ 0 & \frac{2}{3} & 0 \\ 0 & 0 & 0 \end{bmatrix} \mathcal{C}_\mathrm{G}, \quad C = \begin{bmatrix} 0 & 0 & 0 \\ 0 & 0 & 0 \\ 0 & 0 & 1 \end{bmatrix} \mathcal{C}_\mathrm{G}. \tag{44}$$

Here, we have to pay a small price for the fact that throughout, A shifts the weight *symmetrically* to two neighboring sites within their local triangle. To maintain the unitarity conditions in equation (43), the walk must now have a 'lazy' component, i.e. some weight may remain at each site at every update, so that $M \neq 0$. The matrix C shifts weight to the one neighbor outside those triangles, as illustrated in figure 4. These weights are the three complex components of the state vector at each site, $\psi_{x,t}$, which are all zero at $t = 0$, except for $x = 0$, where $\psi_{0,0} = \psi_{IC}$ is arbitrary but normalized, $|\psi_{IC}^2| = 1$. These weights are mixed via $\mathcal{C}_\mathrm{G}$ at each site before a shift entangles them within the network.

Iterating the RG-recursions in equation (40) for the matrices in equation (44) for only $k = 2$ steps already reveals a simple recursive pattern that suggests the ansatz

$$M_k = \begin{bmatrix} \frac{a_k - 2b_k}{3} & \frac{a_k - 2b_k}{3} + \frac{3z+1}{3/z+1} & 0 \\ \frac{a_k - 2b_k}{3} + \frac{3z+1}{3/z+1} & \frac{a_k - 2b_k}{3} & 0 \\ 0 & 0 & 0 \end{bmatrix} \mathcal{C}_\mathrm{G}, \quad A_k = \begin{bmatrix} \frac{a_k + b_k}{3} & \frac{a_k + b_k}{3} & 0 \\ \frac{a_k + b_k}{3} & \frac{a_k + b_k}{3} & 0 \\ 0 & 0 & 0 \end{bmatrix} \mathcal{C}_\mathrm{G}, \tag{45}$$

while $C_k = C_0 = zC$ does not renormalize. Inserted into the RG-recursions in section 3.1, these matrices exactly reproduce themselves *in form* after one iteration, $k \to k+1$, when we identify for the scalar RG-flow:

$$a_{k+1} = \frac{(9z^3 + 5z^2 - 5z - 9)(a_k - 2b_k) - 6(3z^2 + 10z + 3)a_k b_k}{3(9z^3 + 5z^2 - 5z - 9) + 2(3z^2 + 10z + 3)(2a_k - b_k)},$$

$$b_{k+1} = \frac{\begin{array}{c} 4(3+z)(9 - 4z - 14z^2 + 6z^3 + 27z^4)(2a_k - b_k)b_k - 12(3+z)^2(9z^2 - 1)a_k b_k^2 \\ -(z^2-1)(9 - 10z + 9z^2)(9 + 14z + 9z^2)(a_k - 2b_k) - 24z(3+z)^2 b_k^2 \end{array}}{\begin{array}{c} 4(3+z)(9 - 10z - 16z^2 + 6z^3 + 27z^4)a_k + 3(z^2-1)(9 - 10z + 9z^2)(9 + 14z + 9z^2) \\ -8(3+z)(9 + 8z - 10z^2 + 6z^3 + 27z^4)b_k - 4(3+z)^2(9z^2 - 1)(2a_k - b_k)b_k \end{array}}. \tag{46}$$

J. Stat. Mech. (2018) 033103

This flow is initiated at $k=1$ with

$$a_{k=1} = \frac{z(z-1)\left(9+22z+9z^2\right)}{(3+z)\left(9+2z-3z^2\right)}, \qquad b_{k=1} = \frac{z(1+z)\left(9+4z+6z^2+4z^3+9z^4\right)}{(3+z)\left(9+2z+4z^2-2z^3+3z^4\right)}. \tag{47}$$

Inserting equation (45) into equation (42), we then also have an expression for the observable X_k in terms of the hopping parameters a_k and b_k. Here, of course, we do not have any closed-form solution of the RG-flow in equation (46). We can merely verify numerically, with a few iterations of the RG-flow, that the Laplace-poles of the hopping parameters, as well as of the observable, behave in a similar manner to those for the Grover-coin walk on the *1d*-line (see figure 3). Thus, in the case of the DSG, we only have the RG to rely on.

3.2.1. Fixed-point analysis. We now proceed to study the fixed-point properties of the RG-flow at $k \sim k+1 \to \infty$. Equation (46) has a non-trivial fixed point for $a_\infty(z) = \frac{(1-z)\left(9+14z+9z^2\right)}{2(z+3)(3z-1)}$ and $b_\infty(z) = \frac{(1+z)\left(9-10z+9z^2\right)}{2(z+3)(3z-1)}$. Due to the choice of a_k and b_k in equation (45), the Jacobian matrix $J_\infty = \left.\frac{\partial(a_{k+1},b_{k+1})}{\partial(a_k,b_k)}\right|_{k\to\infty}$ of the fixed point is already diagonal and z-independent, with two eigenvalues, $\lambda_1 = 3$ and $\lambda_2 = \frac{5}{3}$, reproducing via equation (14) the already known result for the quantum walk dimension of the DSG with a Grover coin, $d_{\mathrm{w}}^{Q} = \log_2\sqrt{5}$ [19]. Extending the expansion of equation (46) in powers of $\zeta = z - z_{\mathrm{FP}}$ for some unspecified fixed-point value z_{FP} for $k\to\infty$ to higher order, we obtain:

$$\begin{aligned} a_k(z) &\sim a_\infty(z_{\mathrm{FP}}) + \zeta^1\mathcal{A}\lambda_1^k + \zeta^2\alpha_k^{(2)} + \zeta^3\alpha_k^{(3)} + \ldots, \\ b_k(z) &\sim b_\infty(z_{\mathrm{FP}}) + \zeta^1\mathcal{B}\lambda_2^k + \ldots, \end{aligned} \tag{48}$$

with unknown constants $\mathcal{A}$ and $\mathcal{B}$, and with

$$\begin{aligned} \alpha_k^{(2)} &\sim c\left(\mathcal{A}\lambda_1^k\right)^2 + \ldots, \\ \alpha_k^{(3)} &\sim c^2\left[\left(\mathcal{A}\lambda_1^k\right)^3 - \frac{1}{2}\left(\mathcal{A}\lambda_1^k\right)^2\left(\mathcal{B}\lambda_2^k\right)\right] + \ldots, \end{aligned} \tag{49}$$

with $c = \left(9z_{\mathrm{FP}}^2 - 1\right)/\left(8z_{\mathrm{FP}}\right)$, where we have only retained leading-order terms in k that contribute to leading order in large k. Note that z_{FP} has no effect on the scaling and merely contributes numerically for any choice of z_{FP} on the unit-circle, irrespective of the location of any poles. Inserting equations (45) and (48) into X_k in equation (42) and expanding (some generic component of X_k) in powers of $\zeta = z - z_{\mathrm{FP}}$ yields

$$\begin{aligned} [X_k]_{11} \sim &-\zeta^{-1}\frac{z_{\mathrm{FP}}+3}{12\left(3z_{\mathrm{FP}}+1\right)\left(\mathcal{A}\lambda_1^k\right)} - \zeta^0\left[\frac{\left(z_{\mathrm{FP}}+3\right)\left(3-25z_{\mathrm{FP}}-3z_{\mathrm{FP}}^2+9z_{\mathrm{FP}}^3\right)}{96z_{\mathrm{FP}}\left(z_{\mathrm{FP}}^2-1\right)}\right] \\ &-\zeta^1\left[\frac{5\left(z_{\mathrm{FP}}+3\right)\left(3z_{\mathrm{FP}}-1\right)^2\left(3z_{\mathrm{FP}}+1\right)}{1536z_{\mathrm{FP}}^2}\left(\mathcal{B}\lambda_2^k\right)\right] + \ldots, \\ &\sim \zeta^{-1}O\left(\frac{1}{\lambda_1^k}\right) + \zeta^0 O(1) + \zeta^1 O\left(\lambda_2^k\right) + \ldots. \end{aligned} \tag{50}$$

J. Stat. Mech. (2018) 033103

While this result reproduces those from [7], it is remarkable that in this case we have to exclude the values $z_{\rm FP} = \pm 1$, although those seem to be squarely inside the domain of poles (see figure 3).

3.3. RG-analysis for a quantum walk with a non-reflective coin

Here, we follow the script from the previous section, except that the quantum walk in this case is driven by the non-reflective coin $\mathcal{C}_{60}$ in equation (8). In this way, we can scrutinize some of the analytic features we found in previous sections. However, it is also the first attempt to assess the impact that the reflectivity of coins has on the evolution of a quantum walk in a non-trivial geometry. Does symmetry breaking in such an internal degree of freedom affect the universality, as would be expressed in a change of the walk dimension $d_{\rm w}^{Q}$ in equation (1), for example?

Again, we investigate the properties of the RG-recursion of section 3 for $\{M, A, C\}$. In the unrenormalized ('raw') description of the walk, these hopping matrices are

$$M = \begin{bmatrix} -\frac{1}{3} & 0 & 0 \\ 0 & -\frac{1}{3} & 0 \\ 0 & 0 & 0 \end{bmatrix} \mathcal{C}_{60}, \quad A = \begin{bmatrix} \frac{2}{3} & 0 & 0 \\ 0 & \frac{2}{3} & 0 \\ 0 & 0 & 0 \end{bmatrix} \mathcal{C}_{60}, \quad C = \begin{bmatrix} 0 & 0 & 0 \\ 0 & 0 & 0 \\ 0 & 0 & 1 \end{bmatrix} \mathcal{C}_{60}, \tag{51}$$

the same matrices as in equation (44), except for the change of coin. We need to iterate the RG-recursions in equation (40) for the matrices in equation (51) for only $k = 2$ steps to find a recursive pattern:

$$M_k = \left(\frac{a_k - 2b_k}{3} \begin{bmatrix} 1 & \frac{3-2z}{z-6} & 0 \\ \frac{z-6}{3-2z} & 1 & 0 \\ 0 & 0 & 0 \end{bmatrix} + \begin{bmatrix} 0 & \frac{z(1-6z)}{z-6} & 0 \\ \frac{z(2-3z)}{2z-3} & 0 & 0 \\ 0 & 0 & 0 \end{bmatrix} \right) \mathcal{C}_{60}, \quad A_k = \frac{a_k + b_k}{3} \begin{bmatrix} 1 & \frac{3-2z}{z-6} & 0 \\ \frac{z-6}{3-2z} & 1 & 0 \\ 0 & 0 & 0 \end{bmatrix} \mathcal{C}_{60}, \tag{52}$$

and $C_k = C_0 = zC$, as before. Inserted into the RG-recursions in section 3.1, these matrices again exactly reproduce themselves when we identify the scalar RG-flow:

$$\begin{aligned} a_{k+1} &= \frac{2\,(9z^2 - z + 9)\,(z^2 - 1)\,(a_k - 2b_k) - 3\,(12z^3 - 41z^2 - 23z + 3)\,a_k b_k}{6\,(9z^2 - z + 9)\,(z^2 - 1) + (12z^3 - 41z^2 - 23z + 3)\,(2a_k - b_k)}, \\ b_{k+1} &= \frac{\begin{array}{c} 3\,(3 + 7z - 49z^2 + 12z^3)\,(3 - 23z - 41z^2 + 12z^3)\,a_k b_k^2 + 4\,(z^2 - 1)^2\,(9 - 7z + 9z^2)\,(9 - z + 9z^2)\,(a_k - 2b_k) \\ +4\,(z^2 - 1)\,(27 - 48z - 331z^2 + 208z^3 - 453z^4 + 108z^5)\,(b_k - 2a_k)\,b_k - 24z\,(z^2 - 1)\,(2z - 3)\,(z - 6)\,b_k^2 \end{array}}{\begin{array}{c} (3 - 23z - 41z^2 + 12z^3)\,(3 + 7z - 49z^2 + 12z^3)\,(2a_k - b_k)\,b_k - 12\,(z^2 - 1)^2\,(9 - 7z + 9z^2)\,(9 - z + 9z^2) \\ -4\,(z^2 - 1)\,(27 - 12z - 361z^2 + 212z^3 - 453z^4 + 108z^5)\,(a_k - 2b_k) - 48z\,(z^2 - 1)\,(2z - 3)\,(z - 6)\,b_k \end{array}} \end{aligned} \tag{53}$$

now initialized by

$$a_{k=1} = \frac{z(z-1)\,(9 - 17z + 9z^2)}{27 - 30z + 14z^2 - 3z^3}, \qquad b_{k=1} = \frac{z(z^2 - 1)\,(9 - 8z - 15z^2 - 8z^3 + 9z^4)}{-27 - 24z + 16z^2 + 28z^3 - 8z^5 + 3z^6}. \tag{54}$$

For the observable X_k, defined in equation (42), we iterate the RG-recursions in section 3.1 symbolically as a function of z up to $k = 6$, and numerically determine the poles of the hopping parameters (all of which have a common denominator) and of X_k. These are again plotted in figure 3. These Laplace-poles share the clustering in the fractalized domains already observed for the DSG with the Grover coin; however, these domains do not include the real-z axis, similar to when using the same non-reflective coin $\mathcal{C}_{60}$ on a *1d*-line. Drawing on both of these cases as reference, we need not worry about a specific choice of a fixed point $z_{\rm FP}$ and whether it is close to $z = \pm 1$. A generic

J. Stat. Mech. (2018) 033103

fixed-point analysis should suffice to uniquely determine the universality class of this quantum walk.

3.3.1. Fixed-point analysis. Here, the fixed-point properties of the RG-flow in equation (46) have a non-trivial fixed point for $a_\infty(z) = \frac{2\left(1-z^2\right)\left(9-z+9z^2\right)}{3-23z-41z^2+12z^3}$ and $b_\infty(z) = \frac{2\left(z^2-1\right)\left(9-7z+9z^2\right)}{3+7z-49z^2+12z^3}$. As before, a_k and b_k in equation (45) were chosen so that the Jacobian matrix J_∞ is diagonal, with the same two eigenvalues, $\lambda_1 = 3$ and $\lambda_2 = \frac{5}{3}$, obtained for the Grover coin. Thus, breaking the coin's reflectivity appears to leave the universality class of this quantum walk unaffected, as expressed by d_{w}^Q.

Extending the expansion of equation (46) in powers of $\zeta = z - z_{\mathrm{FP}}$ for some unspecified fixed-point value z_{FP} for $k \to \infty$ to higher order, we again obtain equations (48)–(49) but with pre-factor

$$c = \frac{\left(3 + 7z_{\mathrm{FP}} - 49z_{\mathrm{FP}}^2 + 12z_{\mathrm{FP}}^3\right)\left(3 - 23z_{\mathrm{FP}} - 41z_{\mathrm{FP}}^2 + 12z_{\mathrm{FP}}^3\right)}{32z_{\mathrm{FP}}\left(1 - z_{\mathrm{FP}}^2\right)\left(2z_{\mathrm{FP}} - 3\right)\left(z_{\mathrm{FP}} - 6\right)}. \tag{55}$$

However, here already the expansion around the fixed point excludes $z_{\mathrm{FP}} = \pm 1$, both being outside the domain of poles (see figure 3). Inserting these results into X_k in equation (42) and expanding in powers of $\zeta = z - z_{\mathrm{FP}}$ yields for some generic component:

$$\begin{aligned}
[X_k]_{11} \sim & -\zeta^{-1}\frac{\left(z_{\mathrm{FP}} - 6\right)\left(2z_{\mathrm{FP}} - 3\right)\left(5 - z_{\mathrm{FP}} - 3z_{\mathrm{FP}}^2\right)\left(3 + z_{\mathrm{FP}} - 5z_{\mathrm{FP}}^2\right)}{3\left(3 - 23z_{\mathrm{FP}} - 41z_{\mathrm{FP}}^2 + 12z_{\mathrm{FP}}^3\right)^2\left(\mathcal{A}\lambda_1^k\right)} - \zeta^0\frac{\left(45 + 72z_{\mathrm{FP}} - 107z_{\mathrm{FP}}^2 - 24z_{\mathrm{FP}}^3 + 45z_{\mathrm{FP}}^4\right)}{96z_{\mathrm{FP}}\left(z_{\mathrm{FP}}^2 - 1\right)} \\
& - \zeta^1\left[\frac{5\left(5 - z_{\mathrm{FP}} - 3z_{\mathrm{FP}}^2\right)\left(3 + z_{\mathrm{FP}} - 5z_{\mathrm{FP}}^2\right)\left(3 + 7z_{\mathrm{FP}} - 49z_{\mathrm{FP}}^2 + 12z_{\mathrm{FP}}^3\right)^2}{6144z_{\mathrm{FP}}^2\left(z_{\mathrm{FP}} - 6\right)\left(z_{\mathrm{FP}}^2 - 1\right)^2\left(2z_{\mathrm{FP}} - 3\right)}\left(\mathcal{B}\lambda_2^k\right)\right] + \ldots, \\
\sim & \, \zeta^{-1}O\left(\frac{1}{\lambda_1^k}\right) + \zeta^0 O(1) + \zeta^1 O\left(\lambda_2^k\right) + \ldots.
\end{aligned} \tag{56}$$

As before, we have to exclude the values $z_{\mathrm{FP}} = \pm 1$. Thus, we obtain the same result for the scaling in X_k as for the Grover coin in equation (50), further affirming that the universality class remains unchanged.

4. Conclusion

We have explored the properties of the RG applied to discrete-time (coined) quantum walks for an alternative coin that breaks the reflection symmetry of the conventional Grover coin. To that end, we have first explored its effect in the exactly solvable case of such walks on a *1d*-line. There, we were able to show by explicit computation that the formal RG fixed-point analysis is generic and unaffected by the specific value of the Laplace parameter $z = z_{\mathrm{FP}}$ at which the analysis is conducted, as long as certain isolated values are excluded. (We note that certain *correlated* limits of the scalar parameters $\vec{a}_k$ also exist for which non-generic, specifically classical random walk, results are obtained, as already indicated in [17]. These also occur at isolated points in z, which we will discuss elsewhere and which do not contradict the generic picture we have presented here.) While the corresponding classical RG analysis is focused on Laplace poles near the real axis at $z \to z_{\mathrm{FP}} = 1$, we have shown that it is necessary to consider fixed points z_{FP} anywhere on the complex unit-circle, as those poles cluster there in

J. Stat. Mech. (2018) 033103

distinct domains. Particularly for the case of a non-reflective coin, these domains may in fact exclude the real axis of the complex z-plane. Yet, despite those variations in the RG-analysis between distinct coins, the universality classes of the quantum walks studied here remain unchanged when reflection symmetry is broken by $\mathcal{C}_{60}$. Here, those classes seem to depend only on the network that is studied, i.e. the *1d*-line and the DSG. In the future, it would be desirable to design families of unitary but non-reflective coins to obtain more general statements regarding universality. Based on the current study, it appears unnecessary to consider specific observables to determine d_{w}^{Q}, as in all cases we found equation (14) satisfied. Hence, it may suffice to merely assume that that equation holds and reduce the calculations to that of the fixed-point Jacobian for the hopping parameters. Still, when considering less-symmetric coins, the biggest algebraic hurdle is to extract a manageable parametrization of the RG-recursions, as in equation (52) for example.

References

[1] Aharonov Y, Davidovich L and Zagury N 1993 *Phys. Rev.* A **48** 1687
[2] Meyer D A 1996 *J. Stat. Phys.* **85** 551
[3] Aharonov D, Ambainis A, Kempe J and Vazirani U 2001 *Proc. 33rd Annual ACM Symp. Theory of Computing* (New York: ACM) pp 50–9
[4] Kempe J 2003 *Contemp. Phys.* **44** 307
[5] Portugal R 2013 *Quantum Walks and Search Algorithms* (Berlin: Springer)
[6] Boettcher S, Li S and Portugal R 2017 *J. Phys. A: Math. Theor.* **50** 125302
[7] Boettcher S and Li S 2018 *Phys. Rev.* A **97** 012309
[8] Shlesinger M F and West B J (ed) 1984 *Random Walks and Their Applications in the Physical and Biological Sciences* (New York: American Institute of Physics)
[9] Weiss G H 1994 *Aspects and Applications of the Random Walk* (Amsterdam: North-Holland)
[10] Hughes B D 1996 *Random Walks and Random Environments* (Oxford: Oxford University Press)
[11] Metzler R and Klafter J 2004 *J. Phys. A: Math. Gen.* **37** R161
[12] Boettcher S, Li S, Fernandes T D and Portugal R 2017 in preparation (arXiv:1708.05339)
[13] Havlin S and Ben-Avraham D 1987 *Adv. Phys.* **36** 695
[14] Boettcher S and Gonçalves B 2008 *Europhys. Lett.* **84** 30002
[15] Plischke M and Bergersen B 1994 *Equilibrium Statistical Physics* 2nd edn (Singapore: World Scientifc)
[16] Redner S 2001 *A Guide to First-Passage Processes* (Cambridge: Cambridge University Press)
[17] Boettcher S, Falkner S and Portugal R 2013 *J. Phys.: Conf. Ser.* **473** 012018
[18] Boettcher S, Falkner S and Portugal R 2014 *Phys. Rev.* A **90** 032324
[19] Boettcher S, Falkner S and Portugal R 2015 *Phys. Rev.* A **91** 052330
[20] Grover L K 1997 *Phys. Rev. Lett.* **79** 325
[21] Inui N, Konno N and Segawa E 2005 *Phys. Rev.* E **72** 056112
[22] Falkner S and Boettcher S 2014 *Phys. Rev.* A **90** 012307
[23] Grimmett G, Janson S and Scudo P F 2004 *Phys. Rev.* E **69** 026119
[24] Konno N 2005 *J. Math. Soc. Japan* **57** 1179